Catalysis Today 148 (2009) 49–54

Contents lists available at ScienceDirect

Catalysis Today

journal homepage: www.elsevier.com/locate/cattod

Preparation and characterization of Pt/HMFI–SBA-15 hybrid catalyst for tetralin transformation

R. Contreras [a], J. Ramírez [a], R. Cuevas-García [a,*], A. Gutiérrez-Alejandre [a], P. Castillo-Villalón [a], G. Macías [a], Iván Puente-Lee [b]

[a] UNICAT, Depto. de Ing. Química, Facultad de Química, UNAM, Cd. Universitaria, 04510 México, D.F., Mexico
[b] USAI, Facultad de Química, UNAM, Cd. Universitaria, 04510 México, D.F., Mexico

ARTICLE INFO

Article history:
Available online 21 August 2009

Keywords:
HMFI–SBA-15 hybrid material
Pt/HMFI–SBA-15 catalyst
Tetralin
Hydrogenation
Ring contraction
Dehydrogenation

ABSTRACT

A Pt catalyst supported on a hybrid material, HMFI–SBA-15, was prepared. Both, support and catalyst (Pt/HMFI–SBA-15) were characterized by nitrogen physisorption, small and wide (2θ) angle XRD patterns, FT-IR, SEM and HRTEM. The acidic properties of the hybrid material were studied by cumene dealkylation and those of the catalyst were studied by FT-IR of adsorbed pyridine. The catalyst, Pt/HMFI–SBA-15, was tested for tetralin transformation at various reaction temperatures 498, 523, 548, 573, 585 and 598 K. Wide-angle XRD and FT-IR in the skeletal region indicate the presence of MFI zeolite fragments incorporated onto SBA-15. The characterization of the acid sites on the support by cumene dealkylation and FT-IR pyridine adsorption revealed the presence of Brönsted acid sites related to the HMFI zeolite fragments in the hybrid materials. For the catalyst, a homogeneous distribution of Pt clusters was found by HRTEM. In the transformation of tetralin, at all the reaction temperatures, the main products were trans + cis-decalins. However, at high reaction temperature ring contraction to spirodecane and dehydrogenation to naphthalene were observed. At 598 K, a maximum of 8% of ring contraction products was obtained.

1. Introduction

Today, the refinery industry faces the need to fulfill environmental regulations, which restrains the content of aromatic compounds in transport fuels and at the same time, the requirement of processing heavier oils, which produce greater amounts of highly aromatic refinery streams such as the light cycle oil (LCO) fraction. To increase the cetane number of LCO and be able to use it in higher proportion as a component of the diesel fraction, it is necessary to treat this stream with a catalyst able to perform hydrogenation and selective ring opening, as suggested by McVicker et al. [1]. For example: the cetane number for naphthalene is 5, compared to 15 for tetralin, 35 for cis- and trans-decalins, and 50 for butyl-benzene. Therefore, the cetane number of aromatic streams can be increased significantly by successive and/or parallel hydrogenation (HYD) and ring-opening (RO) reactions. However, it has been established that selective ring opening leading to compounds with high cetane number is not an easy task to achieve, especially when dealing with the partially hydrogenated products of naphthalene and phenanthrene [2].

It is well known, that the saturation of aromatic hydrocarbons is performed with noble metals like metallic Pt, at low temperature and high pressure [3]. Concerning the ring-opening reactions, Gault found that the selective ring opening for methylcyclopentane to the corresponding C_6 paraffins can be made using: Pt, Pd, Ir, Ru and Rh catalysts supported on alumina [4]. McVicker et al. [1] demonstrated, using an Ir/Al_2O_3 catalyst, that ring opening activity for alkyl-cyclohexanes is lower than for alkyl-cyclopentanes and suggested the use of an acidic function to isomerize the C_6 rings to methyl-C_5 ring (ring contraction, RC) and in this way facilitate the formation of the corresponding paraffin. Arribas et al. [5,6], using Pt/USY and Pt/ITQ catalysts, evidenced that the ring opening of tetralin involves three steps: (a) hydrogenation of tetralin to cis/trans-decalins on a metallic site, (b) ring contraction from decalins to methylperhydroindanes, which requires an acid site, and (c) ring-opening reactions to transform methylperhydroindanes to alkyl-cycloalkanes on a metal site. However, some contribution to the cetane number is lost because alkyl-cycloalkanes undergo considerable dealkylation (~20%) and cracking, due to the strength of the zeolite acid sites. In another work, Carrión et al. [7] studied the transformation of tetralin over PtPd/ZrMCM-41; their results indicated good hydrogenation with poor hydrogenolysis/ring opening activity; showing that the acidity of Zr-modified MCM-41 was not enough to lead to RO products, although the authors

* Corresponding author. Tel.: +52 55 56225968; fax: +52 55 56225366.
E-mail address: cuevas@unam.mx (R. Cuevas-García).

0920-5861/$ – see front matter © 2009 Elsevier B.V. All rights reserved.
doi:10.1016/j.cattod.2009.06.023

reported the presence of some hydrocracking products. It appears then that better performance can be achieved with a catalytic system where the acidic function is not too strong to lead to undesirable hydrocracking products (HYC) but strong enough to allow ring contraction reactions.

Products and reactant diffusion restrictions can be avoided using mesoporous materials, like SBA-15. The lack of surface acidity of the siliceous framework can be circumvented by incorporating an acidic material like a zeolite into the matrix or on the internal surface of SBA-15. Improvement of both the stability and acidity of SBA-15 can be achieved by incorporating some zeolite-like order onto the pore walls [8]. Recently, it was shown that the walls of the mesostructure can be converted to a partially zeolitic product, yielding a new type of materials, with semicrystalline zeolitic mesopore walls synthesized from the amorphous walls of SBA-15 [9]. These kind of materials are interesting since they would exhibit the properties of both zeolites and mesoporous solids.

In this work, HMFI zeolite fragments were incorporated into the porous system of SBA-15, following a procedure reported previously [9]. Platinum was supported on the HMFI–SBA-15 material, and the resulting bifunctional Pt/HMFI–SBA-15 catalyst was tested in the transformation of tetralin to analyze its performance in the hydrogenation, ring contraction and ring-opening reactions.

2. Experimental

2.1. Preparation of HMFI–SBA-15

The HMFI–SBA-15 hybrid material was synthesized in three steps: (a) synthesis of SBA-15; (b) incorporation of MFI zeolite fragments on the SBA-15 pore walls; and (c) transformation of the sodic form of MFI to the acid form.

(a) SBA-15 was synthesized following the method reported previously by Zhao et al. [10]. (b) MFI-SBA-15 was prepared by coating the SBA-15 support with a zeolitic seed, following the procedure reported by Trong On and Kaliaguine [9] and Campos et al. [11]. Briefly, for the preparation of the diluted zeolite gel, anhydrous sodium aluminate (Sigma–Aldrich CAS No. 11138-49-1), tetrapropylamonium hydroxide (TPAOH), 1.0 M solution in water (Sigma–Aldrich), and tetraethyl orthosilicate (TEOS) 98% purity (Sigma–Aldrich CAS 78-10-4), were used as reactants. For the synthesis, a solution consisting of 7 g of tetrapropylamonium hydroxide (TPAOH) and 3.9 g of TEOS was mixed with another solution containing 0.2191 g of sodium aluminate dissolved in 5 g of deionized water. The resulting solution was stirred for 24 h at room temperature and then diluted with deionized water to a volume of 150 mL. SBA-15 was contacted with this solution for 1 h. The solid was dried overnight at 328 K. The dried solid was poured into an autoclave reactor containing glycerol (19 g) and water (8 g). The reactor was maintained at 423 K for 3 h. Then the product, NaMFI-SBA-15, was filtered, washed with deionized water, dried at room temperature and finally calcined at 823 K for 6 h.

(c) To transform the NaMFI-SBA-15 to its acid form, HMFI–SBA-15, the procedure proposed by Frunz et al. [12] was used: 2 g of MFI-SBA-15 were contacted with a solution of 0.5 g of NH_4NO_3 in 200 mL of ethanol at 333 K for 1 h the solid was then dried at room temperature and calcined at 823 K for 5 h.

2.2. Catalysts preparation

The catalyst Pt/HMFI–SBA-15 was prepared by ion exchange using a solution of tetra-ammine platinum (II) nitrate, 99% purity from Strem Chemicals (CAS no. 20634-12-2). Typically, 1.98 g of HMFI–SBA-15 were contacted with the platinum solution to form a slurry, maintaining the pH of 8, the slurry was stirred for 3 h at room temperature and filtered. The resulting solid was calcined in oxygen flow (300 mL/min) at 673 K for 2 h.

2.3. Characterization

The surface and porosities of SBA-15, HMFI–SBA-15 and Pt/HMFI–SBA-15 were characterized by nitrogen physisorption using a Micromeritics TriStar SAPA equipment; before each measure the sample was outgassed at 543 K in vacuum for 24 h.

XRD patterns for pure SBA-15, MFI-SBA-15 and Pt/HMFI–SBA-15 were collected at low $2^\circ \leq 2\theta \leq 4^\circ$, and wide $5^\circ \leq 2\theta \leq 50^\circ$ angles on a Siemens D5000 diffractometer using Cu Kα (λ = 1.5406 Å) radiation.

SEM analyses for SBA-15, HMFI–SBA-15 and Pt/HMFI–SBA-15 were carried out using a Jeol JSM-5900LV microscope equipped with an EDX-ISIS Oxford detector. HRTEM observations for SBA-15, MFI-SBA-15 and Pt/HMFI–SBA-15, were carried out using a Jeol 2010 microscope operating at 200 kV with 1.9 Å point-to-point resolution.

The cumene dealkylation reaction using N_2 as carrier gas in a microreactor operating at 573 K and atmospheric pressure was used to characterize the acid sites of SBA-15 and HMFI–SBA-15. Pyridine adsorption was used to corroborate the presence of Brönsted acid sites in Pt/HMFI–SBA-15. A self-supported wafer of the catalyst placed in the IR cell was pretreated at 613 K for 3 h in oxygen flow. Then the sample was cooled down to room temperature before introducing pyridine pulse. The physisorbed pyridine was eliminated by outgassing the sample at room temperature. Finally, the IR spectrum was registered at room temperature and at T = 373, 473 and 573 K. All the spectra were collected with a Nicolet FT-IR Magna 760 using 2 cm^{-1} resolution and 100 scans per spectrum.

2.4. Catalytic activity test

Prior to the tetralin transformation, the oxide Pt/HMFI–SBA-15 was reduced *in situ* under H_2 flow at 673 K for 4 h. The possible reactions over the reduced catalyst are: hydrogenation (HYD) of tetralin to cis- and trans-decalins, dehydrogenation (DHYD) to naphthalene, ring contraction reactions (RC) leading to methyl-perhydroindanes, and the undesirable hydrocracking (HYC) reactions.

The transformation of tetralin was conducted in an ISRI HP100 automated flow microreactor apparatus operating in steady-state at 5.5 MPa and WHSV = 100 h^{-1}, isothermally at T = 498, 523, 548, 573, 585 and 598 K. All the activity tests were performed using a feed of 40 wt% tetralin dissolved in cyclohexane. The reaction products were collected every hour, identified with a GC-MS HP 61800B GCD system and quantified with a HP-6890 gas chromatograph. Tetralin conversion (X) and products yield (Y) were calculated as follows:

$$(X) = [(\text{tetralin in feed-tetralin after reaction})/\text{tetralin in feed}] \times 100.$$

$$(Y) = [\text{desired product}/(X)] \times 100, \quad \text{where desired product} = \text{ring contracted or hydrogenated product.}$$

3. Results and discussion

3.1. Characterization results

Fig. 1A shows the low angle ($1^\circ < 2\theta < 4^\circ$) X-ray diffraction pattern for SBA-15 and HMFI–SBA-15. Both materials display

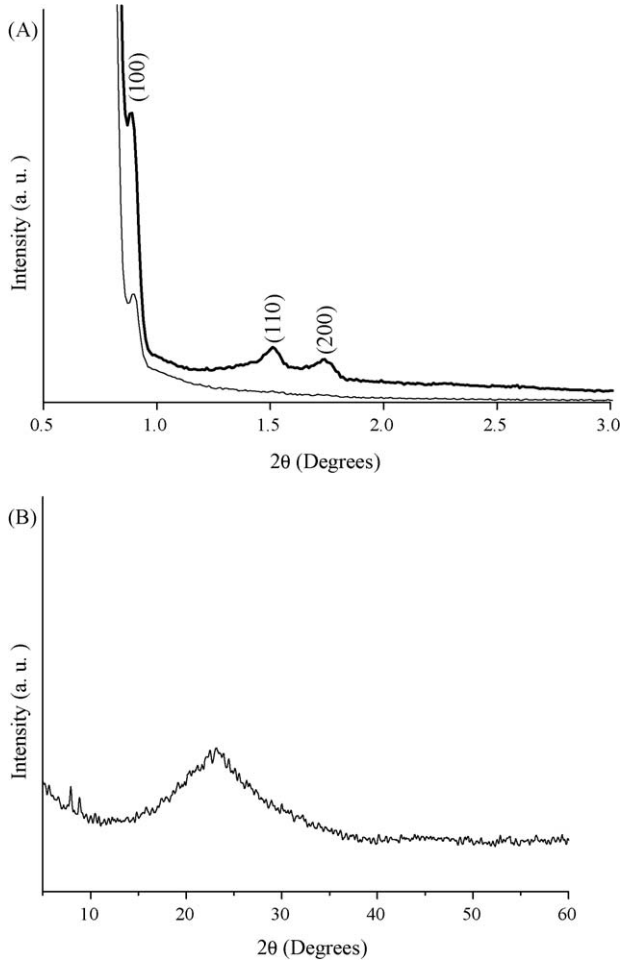

Fig. 1. Low angle XRD patterns (A) for SBA-15 (—) pure and HMFI–SBA-15 (—). XRD wide-angle pattern for HMFI–SBA-15 (B).

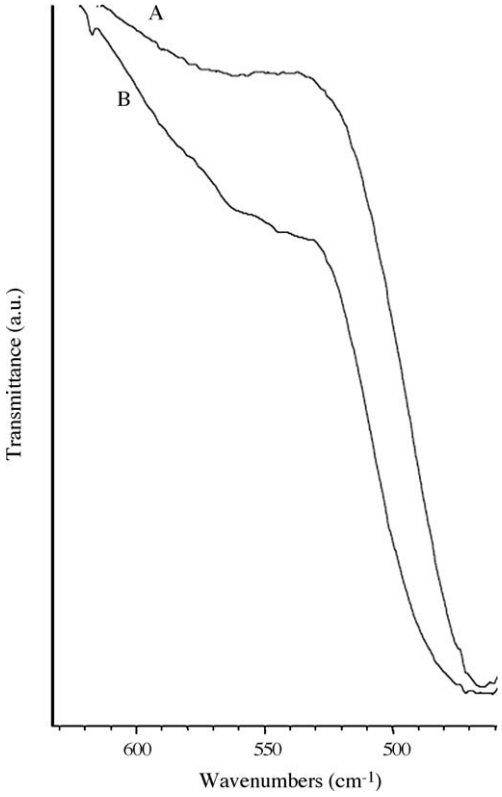

Fig. 2. FT-IR spectra of the skeletal region for SBA-15 (A) and HMFI–SBA-15 (B).

diffraction peaks with Miller indexes (1 0 0), (1 1 0) and (2 0 0) characteristic of the hexagonal porous arrangement of SBA-15 [10]. In the wide-angle XRD patterns (Fig. 1B), small diffraction peaks located at $2\theta = 7.9^\circ$ and 8.9° can be observed, pointing out the presence of zeolite MFI [13]. However, other expected peaks assigned to the MFI structure are not observed probably because they are obstructed by the presence of a very broad reflexion peak approximately at $15^\circ < 2\theta < 30^\circ$, associated with amorphous silica. Another possible reason for absence of these peaks is the low concentration of the MFI fragments present on the SBA-15 internal surface. To corroborate the presence of the MFI, analysis of the FT-IR skeletal lattice vibrations at the 400–700 cm^{-1} region was carried out. According to literature [14,15,9] a band assigned to five membered ring vibrations characteristic of the HMFI structure appears at *ca.* 550 cm^{-1}. The IR spectrum of HMFI–SBA-15 shows the incipient existence of a band around 550 cm^{-1} (Fig. 2), supporting the presence of HMFI structures in agreement with the zeolite peaks observed by XRD. This band is absent in the pure SBA-15 sample.

The SEM micrograph of HMFI–SBA-15 shows grains with uniform morphology of 0.9–1.0 μm sizes (Fig. 3). The micrograph of the catalyst Pt/HMFI–SBA-15, not shown here, displays the same morphology.

The hexagonal arrangement of pores for the pure SBA-15 was confirmed by HRTEM, see Fig. 4A. After HMFI incorporation, Fig. 4B shows the preservation of the channel arrangement of the SBA-15, besides some amorphous particles of non-crystallized silica, are also observed. The micrograph of Pt/HMFI–SBA-15 (Fig. 4C) shows the typical porous hexagonal arrangement of SBA-15 in front and side views. A homogeneous distribution of platinum clusters, 5–7 nm in size, was also observed. The platinum clusters are equal or smaller than the dimensions of the SBA-15 channels (7 nm). Hence, it could be considered that at least part of the Pt clusters is located inside the pores of the HMFI–SBA-15 support.

Analysis of the textural properties showed specific surface areas of 890 and 346 m^2/g for pure SBA-15 and HMFI–SBA-15. The considerable lower value for HMFI–SBA-15 was apparently due to the partial dissolution of SBA-15 during the synthesis procedure of the hybrid material, which takes place under basic conditions (pH ∼ 10). In line with this possibility, some of the dissolved silica were observed in Fig. 4B. Nevertheless, the area of the hybrid support is high enough to proceed to the catalyst preparation. The

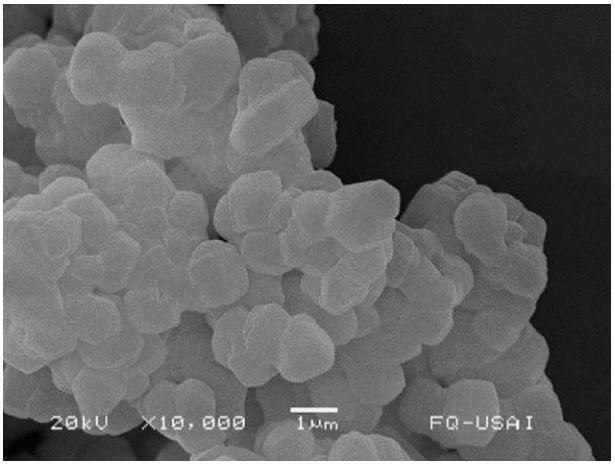

Fig. 3. Micrograph of SEM for HMFI–SBA material.

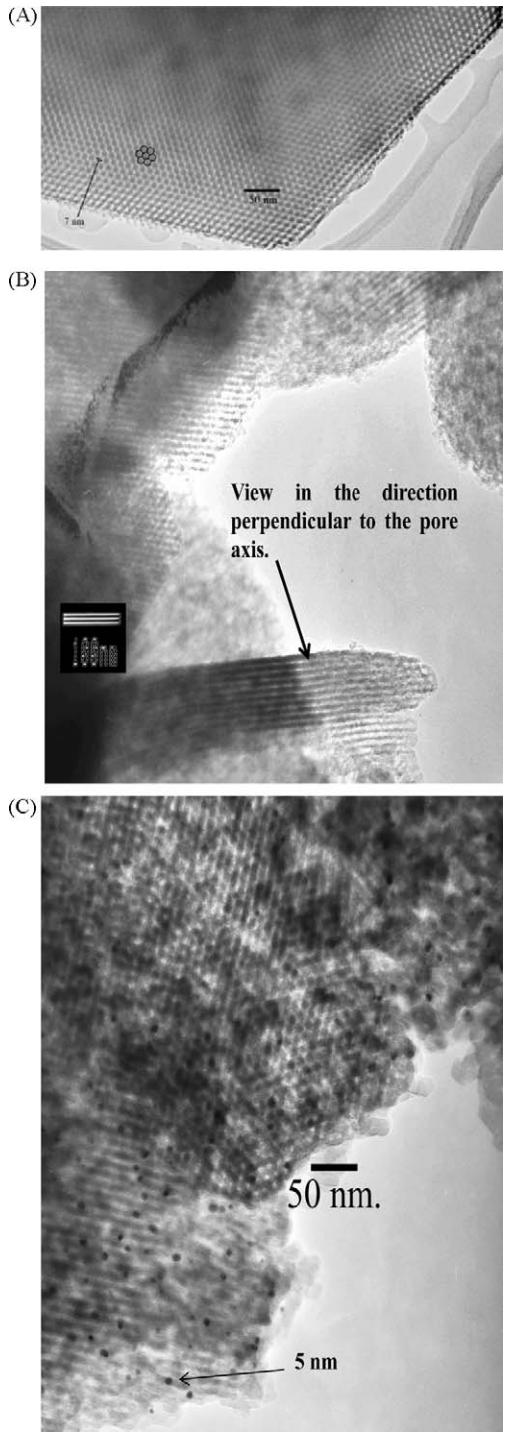

Fig. 4. HRTEM micrographs: SBA-15 pure (A), HMFI–SBA-15 (B) and Pt/HMFI–SBA-15 catalyst (C).

addition of Pt, 2.2 wt.% as determined by SEM-EDX, to HMFI–SBA-15 caused only an additional small decrement in surface area, to yield 306 m^2/g.

To assess the acid properties of the HMFI–SBA-15, the cumene dealkylation reaction was performed; this technique is commonly used to characterize the Brönsted or Lewis acidity of acid solids [16–19]. Benzene and propene are produced on Brönsted acid sites whereas α-methylstyrene is formed on Lewis acid sites. Thus, product selectivity is a measure of the Brönsted/Lewis acid sites ratio. Fig. 5 shows the overall conversion of cumene on HMFI–SBA-15 and two mechanical mixtures, HMFI (2.5 and 5 wt%) + SBA-15

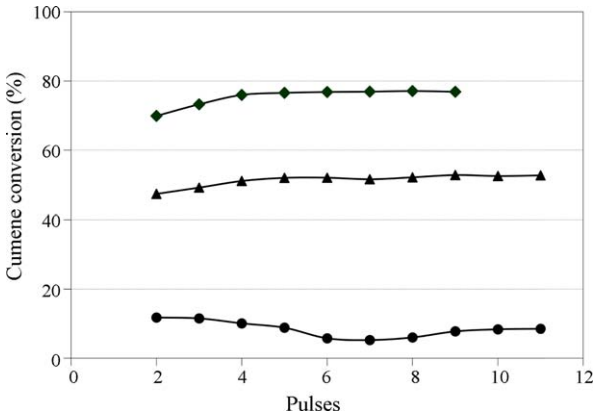

Fig. 5. Overall cumene conversion with HMFI–SBA-15 and two mechanical mixtures. HMFI/SBA-15 (●), HMFI (5%) + SBA-15 (◆), HMFI (2.5%) + SBA-15 (▲), at 573 K, atmospheric pressure, gas carrier N_2.

used as references. The catalytic activity of pure SBA-15 (not shown) was nil due to the absence of acid sites (Lewis and Brönsted). For the mechanical mixtures, high cumene conversions were achieved; here the only detected products, benzene and propene, are associated with the Brönsted acid sites in the zeolite component. Finally, the hybrid material HMFI–SBA-15 presents nearly 10% conversion, the reaction products were, also, benzene and propene, confirming the presence of Brönsted acid sites capable of produce dealkylation reactions.

The IR spectra of pyridine adsorbed on Pt/HMFI–SBA-15 show the presence of three well defined bands located at 1544, 1490 and 1455 cm^{-1} (Fig. 6). The 1544 cm^{-1} band arise from pyridine protonation (Brönsted acidity), the band at 1490 cm^{-1} is due to the adsorption of pyridine on Brönsted and Lewis sites, and the sharp band at 1455 cm^{-1} with a shoulder at 1435 cm^{-1} has been assigned to chemisorbed pyridine on Lewis sites and to hydrogen bonded pyridine on hydroxyls groups, respectively [20,21]. As the outgassing temperature increases, the shoulder (1435 cm^{-1}) disappears and the intensity of the sharp band associated with Lewis acidic sites drastically diminishes. At high outgassing temperature, ≥473 K, a broad band with two maxima (1445 and 1455 cm^{-1}) remains. This behavior suggests that two types of Lewis sites exist on the Pt/HMFI–SBA-15 catalysts. The intensity of the band associated with Brönsted acid sites was not affected despite the high outgassing temperature. These Brönsted acid sites are responsible for the production of benzene and propene.

3.2. Catalytic activity

No extensive hydrocracking of tetralin was detected in the reaction tests. The liquid mass balance was close to 99% in all cases and the mass spectrometry analysis of the evolved gas detected mainly a small quantity of non-condensed cyclohexane (used as solvent) and traces of propane and tetralin. Also, the cumene characterization (*vide supra*) showed the absence of any further product from the hydrocracking of benzene.

A reaction test using Pt/SBA-15 as reference was performed at 548 K, 5.5 MPa of hydrogen pressure. The total tetralin conversion was 22% and the products were almost 100% cis + trans-decalin, no ring contraction or ring opening products were detected.

For Pt/HMFI–SBA-15, the tetralin total conversions in the temperature range 498–598 K started at 28%, achieved a maximum of 76% at 548 K and at the higher temperature (598 K) the conversion was 48% (Fig. 7). Taking into account that the main reaction is HYD to give decalins; but that at the same time tetralin can suffer dehydrogenation to give naphthalene, *vide infra*, the drop in conversion can be explained by the thermodynamic

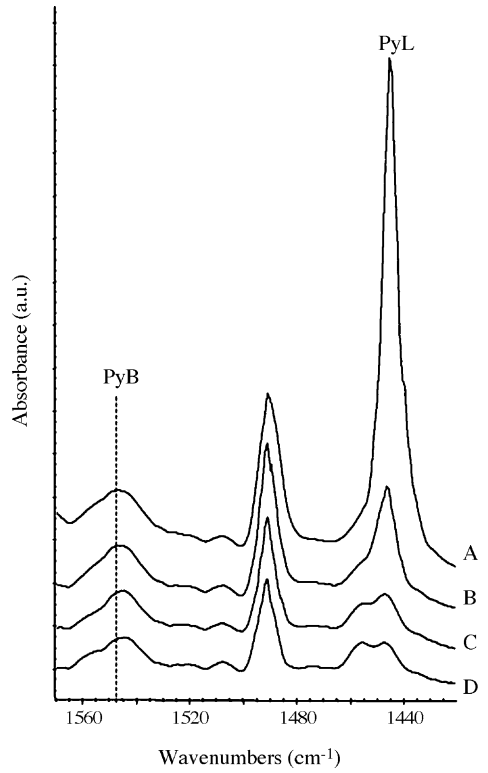

Fig. 6. FT-IR spectra for Pt/HMFI–SBA-15 catalyst with adsorbed pyridine. After outgassing at (A) room temperature, (B) 373 K, (C) 473 K and (D) 573 K.

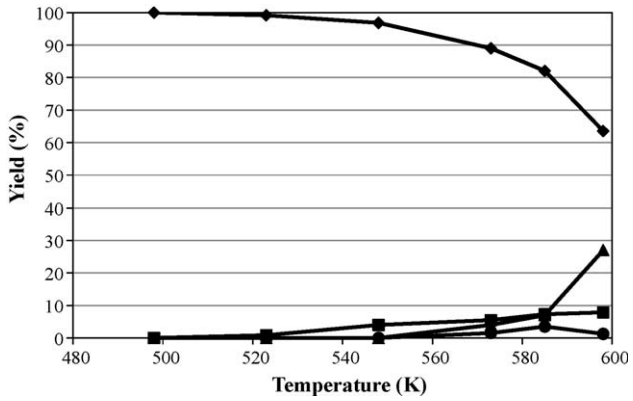

Fig. 8. Yields (%) for hydrogenation products (◆), ring contraction (■), dehydrogenation (▲) and ring opening products (●), at T = 498, 523, 548, 573, 585 and 598 K at 5.5 MPa, WHSV = 100 h^{-1}.

Table 1
Trans-decalin/cis-decalin ratio obtained at T = 498, 523, 548, 573, 585 and 598 K under 5.5 MPa of hydrogen, WHSV = 100 h^{-1}.

Temperature (K)	Trans/cis-decalins ratio
498	0.91
523	2.47
548	2.81
573	4.23
585	4.37
598	3.85

constraints of the exothermic hydrogenation reaction, favored at lower temperatures [22–24].

Fig. 8 presents the yield of the hydrogenation, ring contraction, dehydrogenation and ring-opening reactions with temperature. The main products at 498–548 K were cis- and trans-decalins (the addition of the yields of both decalins was almost 100%), which have a cetane number (CN) about three times that of tetralin. Table 1 shows the trans/cis-decalin ratio versus reaction temperature. At 498 K, the concentration of cis-decalin was higher than that of trans-decalin. Ma et al. [25] observed similar results using Pt/USY catalysts. In contrast, at higher temperatures, from 523 to 598 K, the concentration of trans-decalin was higher than cis-decalin. This tendency can be explained because at high temperature cis-decalin is isomerized to trans-decalin over the acid sites of the catalyst; Dokjampa et al. [26] found a similar result.

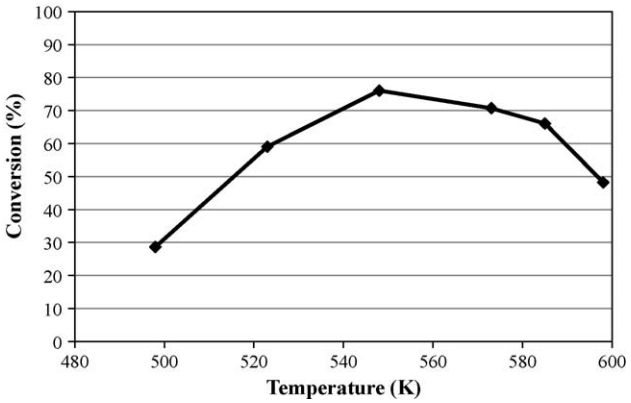

Fig. 7. Overall conversion (%) for tetralin, at T = 498, 523, 548, 573, 585 and 598 K at 5.5 MPa, WHSV = 100 h^{-1}.

At temperatures higher than 548 K, the ring contraction (RC) function was evidenced by the formation of spirodecane and bicyclopentyl; both products coming from decalins. Other detected RC product was methyl-indane, which is produced from direct tetralin ring contraction. The concentrations of RC products increase with temperature; the maximum concentration, ~8% was obtained at 598 K, it is well known that RC is a critical previous step to ring-opening reactions.

As can be seen in Fig. 8, the yields of hydrogenated products diminish from 100% to 70%, as the temperature changes from 573 to 598 K. The yield diminished because the dehydrogenation of tetralin to naphthalene began to occur at 573 and became more relevant as the temperature raised, according to the thermodynamics of the system [22–24]. At the same time, the yield of naphthalene increased from 4.5 to 27 wt% at 573 and 598 K respectively. However, at the higher temperatures some small quantities of ring opening products (decane and alkyl-benzenes) were detected, indicating that the whole sequence of reactions leading to RO took place.

4. Conclusions

The synthesized HMFI–SBA-15 material has Brönsted acid sites associated with the presence of HMFI zeolite fragments on the pore walls of SBA-15. It can be concluded that in the transformation of tetralin, the Pt/HMFI–SBA-15 catalyst can perform: hydrogenation, ring contraction, and ring-opening reactions, producing cis- and trans-decalins (HYD products), spirodecane and methyl-indane (RC products) and, at high temperature, small concentrations of alkyl-benzenes (RO products).

Acknowledgements

R. Contreras acknowledges for the fellowship for his post-graduate studies, CONACyT register number 159343. This work

was supported by the project CONACyT 49479. We thank Cecilia Salcedo for the XRD work.

References

[1] G.B. McVicker, M. Daage, M.S. Touvelle, C.W. Hudson, D.P. Klein, W.C. Baird Jr., B.R. Cook, J.G. Chen, S. Hantzer, D.E.W. Vaughan, E.S. Ellis, O.C. Feeley, J. Catal. 210 (2002) 137.
[2] R.C. Santana, P.T. Do, M. Santikunaporn, W.E. Alvarez, J.D. Taylor, E.L. Sughrue, D.E. Resasco, Fuel 85 (2006) 643.
[3] J. Cosyns, Chapter XVI, The hydrogenation of hydrocarbons. Fundamental and Industrial Aspects of Catalysis by Metals, in: B. Imelik, G.A. Martin, A.J. Renouprez (Eds.), Editions du CNRS, 1984.
[4] F.G.J. Gault, Adv. Catal. 30 (1981) 1.
[5] M.A. Arribas, A. Corma, J.M. Díaz-Cabañas, A. Martínez, Appl. Catal. A 273 (2004) 277.
[6] M.A. Arribas, P. Concepción, A. Martínez, Appl. Catal. A 267 (2004) 111.
[7] M.C. Carrión, B.R. Manzano, F.A. Jalón, D. Eliche-Quesada, P. Maireles-Torres, E. Rodríguez-Castellón, A. Jiménez-López, Green Chem. 7 (2005) 793.
[8] Y. Liu, T.J. Pinnavaia, J. Mater. Chem. 12 (2002) 3179.
[9] D. Trong On, S. Kaliaguine, Angew. Chem. Int. Ed. 113 (2001) 3348.
[10] D. Zhao, J. Feng, Q. Huo, N. Melosh, G.H. Fredrickson, B.F. Chmelka, G.D. Stucky, Science 279 (1998) 548.
[11] A.A. Campos, L. Dimitrov, C.R. da Silva, M. Wallau, E.A. Urquieta-González, Micropor. Mesopor. Mater. 95 (2006) 92.
[12] L. Frunz, R. Prins, G.D. Pirngruber, Micropor. Mesopor. Mater. 88 (2006) 152.
[13] M.M.J. Treacy, J.B. Higgins, Collection of Simulated XRD Powder Patterns for Zeolites, 4th ed., Elsevier, Amsterdam, 2001.
[14] P.A. Jacobs, E.G. Derouane, J. Weitkamp, J. Chem. Soc., Chem. Commun. (1981) 591.
[15] G. Couldurier, C. Naccache, J. Vedrine, J. Chem. Soc., Chem. Commun. (1982) 1413.
[16] A. Corma, B.W. Wojciechowski, Catal. Rev. -Sci. Eng. 24 (1982) 1.
[17] M. Kurian, S. Sugunan, Micropor. Mesopor. Mater. 83 (2005) 25.
[18] T. Chiranjeevi, G.M. Kumaran, J.K. Gupta, G. Murali Dhar, Thermochim. Acta 443 (2006) 87.
[19] J.A. Lercher, A. Jentys, A. Brait in, H.G. Karge (Eds.), 1st ed., Molecular Sieves: Science and Technology, vol. 6, Springer-Verlag, Berlin, 2008, , p. 153Chap. 3.
[20] J. Datka, E. Tuznik, J. Catal. 102 (1986) 43.
[21] S. Bhatia, Zeolite Catalysis: Principles and Applications, CRC Press, Boca Raton, 1990, p. 200, Chap. 8.
[22] W. Qian, Y. Yoda, Y. Hirai, A. Ishihara, T. Kabe, Appl. Catal. A 184 (1999) 81.
[23] M. Sanati, B. Harrysson, M. Faghihi, B. Gevert, S. Järås, in: J.J. Spivey (Ed.), 1st ed., Catalysis, vol. 16, RSC, 2002, p. 30 Chap. 1.
[24] J.F. Le Page, J. Cosyns, P. Courty, E. Freund, J.P. Franck, Y. Jacquin, B. Juguin, C. Marcilly, G. Martino, J. Miquel, R. Montarnal, A. Sugier, H. Van Landeghem, Applied Heterogeneous Catalysis Design, Manufacture and Use of Solid Catalysts, Institut Francais du Pétrole Publications, Paris, 1987, p. 368.
[25] H. Ma, X. Yang, G. Wen, G. Tian, L. Wang, Y. Xu, B. Wang, Z. Tian, L. Lin, Catal. Lett. 116 (2007) 149.
[26] S. Dokjampa, T. Rirksomboon, S. Osuwan, S. Jongpatiwut, D.E. Resasco, Catal. Today 123 (2007) 218.